SCC Colony Crack Shielding Factors Determined Using FEA

Colin Scott and Abu Hena Muntakim
Northern Crescent, Inc.

Pipeline Pigging and Integrity Management Conference

February 12-16, 2024

Organized by
Clarion Technical Conferences

https://doi.org/10.52202/072781-0067

https://doi.org/10.52202/072781-0067

Abstract

Stress corrosion cracks are typically found in colonies comprised of multiple parallel aligned cracks. However, they are usually assessed as individual (or single interlinked) cracks, assuming the deepest of the colony represents the crack driving force for failure. This common approach does not account for the effects of crack shielding. It is known that neighbouring cracks may dissipate stress intensity and result in a lower crack driving force.

In this work we use FEA to estimate the stress intensity factors associated with crack colonies. Results demonstrate how stress intensities in colonies are decreased relative to those of individual cracks. This is consistent with recent industry model studies that tend to underestimate critical failure pressures of in-service SCC flaws. It also indicates a fracture mechanics contribution to the known phenomenon of crack dormancy, which is often attributed to electrochemical and kinetic factors. The findings can be used to modify fitness for service assessments and improve SCC integrity program efficiency.

Introduction

Failure pressure calculations are an important part of all oil and gas pipeline operator's integrity management programs. Analysts must be able to predict the maximum pressure that a pipeline can sustain in service and apply a suitable safety factor to account for uncertainties. Pipelines in service will have known (or unknown) distributions of flaws that must be included in these failure pressure predictions. Flaws may be metal loss, crack-like or deformation. The focus of this paper is crack-like flaws, specifically axial stress corrosion cracks in colonies.

Several failure pressure prediction models are available in the industry standards to assess crack-like flaws; including the original and modified log-secant models, ASME FFS - 1 / API 579, BS 7910, CorLAS™ and PRCI MAT - 8 [1 - 6]. These models have been studied extensively by industry and their failure pressure predictions compared to laboratory tests and in-service failure data [7 - 14].

The failure pressure predictions, and their reliability, have a direct impact on the effectiveness and efficiency of the operator's integrity management programs. If failure pressure predictions are non-conservative, the operator may excavate and repair fewer features than are necessary to maintain pipeline integrity and this could result in an ineffective and unsafe integrity program. However, if failure pressure predictions are overly conservative, the operator may excavate and repair more features than are necessary and this could result in an inefficient and financially costly integrity program.

The models provided in the industry standards have been shown in the literature to be overly-conservative for axial stress corrosion cracking (SCC) failure pressure predictions [10 - 14]. Yan et al [10] demonstrated the most accurate of the industry accepted failure pressure models for SCC is the CorLAS™ model. They reported an accuracy of 1.11 and a standard deviation of 0.15 when detailed crack profiles were considered. In this case, the accuracy is the average of the true failure pressure determined from in-service or hydrotest failures divided by model predicted failure pressures. The other industry accepted crack models were even more conservative. These analyses were performed using direct crack depth measurements from failed pipelines, so sizing error does not play a significant role in the inaccuracy of the predictions.

https://doi.org/10.52202/072781-0067

The authors believe the conservatism in the current failure pressure models is, in part, due to these models disregarding the effect of crack shielding [15 - 16]. A single crack will have a higher stress intensity associated with it, as compared to a crack colony, in which the neighboring parallel cracks dissipate stress intensity and result in a lower crack driving force. The overly conservative failure pressure predictions are a direct result of an over-estimation of the stress intensity factor.

In this work, the authors look at how stress intensity factors differ between single, isolated cracks and SCC colonies. The shielding phenomenon has been studied in the academic literature, but to the authors' knowledge is not being applied explicitly to SCC in the oil and gas pipeline industry. Tada, Paris and Irwin [17] studied stress intensity factors in periodic crack arrays in semi-infinite space and subject to remote uniaxial tension. Their work demonstrated a dependence on both crack depth and crack spacing. The work predicts crack dormancy when the crack depth to spacing ratio reaches 1/3. Parker [18] later demonstrated the crack dormancy phenomenon in several natural systems, including mud-cracking, crevasse formation in glaciers, cooling of basalt columns and environmental cracking in gun tubes. He further demonstrated the phenomenon of "crack-shedding", which allows a subset of cracks in a periodic crack array to continue to propagate, even after dormancy conditions have been satisfied.

The periodic crack array geometry and results reported by Tada are provided in **Figure 1**. Tada provided two forms of the stress intensity "compliance factor" solution. The first follows the conventional form of Irwin's equation.

$$K_I = F_1(s) \cdot \sigma \cdot \sqrt{\pi \cdot a}$$

Where K_I is the mode I stress intensity factor, F_1 the standard compliance factor, σ the applied stress and a the crack depth. Note that the compliance factor is a function of the crack depth to spacing ratio "s", which is defined as s = a/(a+h), with h the crack half - spacing. Tada showed the compliance factor decreases as the crack grows (red highlight in figure). The increasing crack depth and decreasing compliance factor offset when s = 0.4 (or a/2h = 1/3). The result is that crack dormancy is predicted. Tada illustrated this by redefining Irwin's equation in terms of the crack half-spacing rather than the crack depth (green highlight in figure).

$$K_I = F_2(s) \cdot \sigma \cdot \sqrt{h}$$

Where F_2 is the modified compliance factor. Although not intuitive, the Tada modification was necessary for the derivation and clearly demonstrates the crack dormancy predicted by the zero slope in the curve at s = 0.4 (or a/2h = 1/3). The green curve in the figure essentially shows how the stress intensity itself will change during crack growth (as the spacing remains constant).

This work builds on the work of Tada and Parker [17,18], and extends arguments presented by the lead author in recent technical papers [11 - 14]. The stress intensity factor results reported by Tada were specific to a particular geometry, and not directly applicable to SCC in oil and gas pipelines. In this work, stress intensity factors are calculated using finite element analysis (FEA). A periodic crack array (colony) in the external wall of thin-walled pipe subject to internal pressure is considered. The objective is to show the primary characteristics of the Tada and Parker [17,18] work are applicable to SCC, and that these results can lead to improved efficiency in pipeline integrity programs.

https://doi.org/10.52202/072781-0067

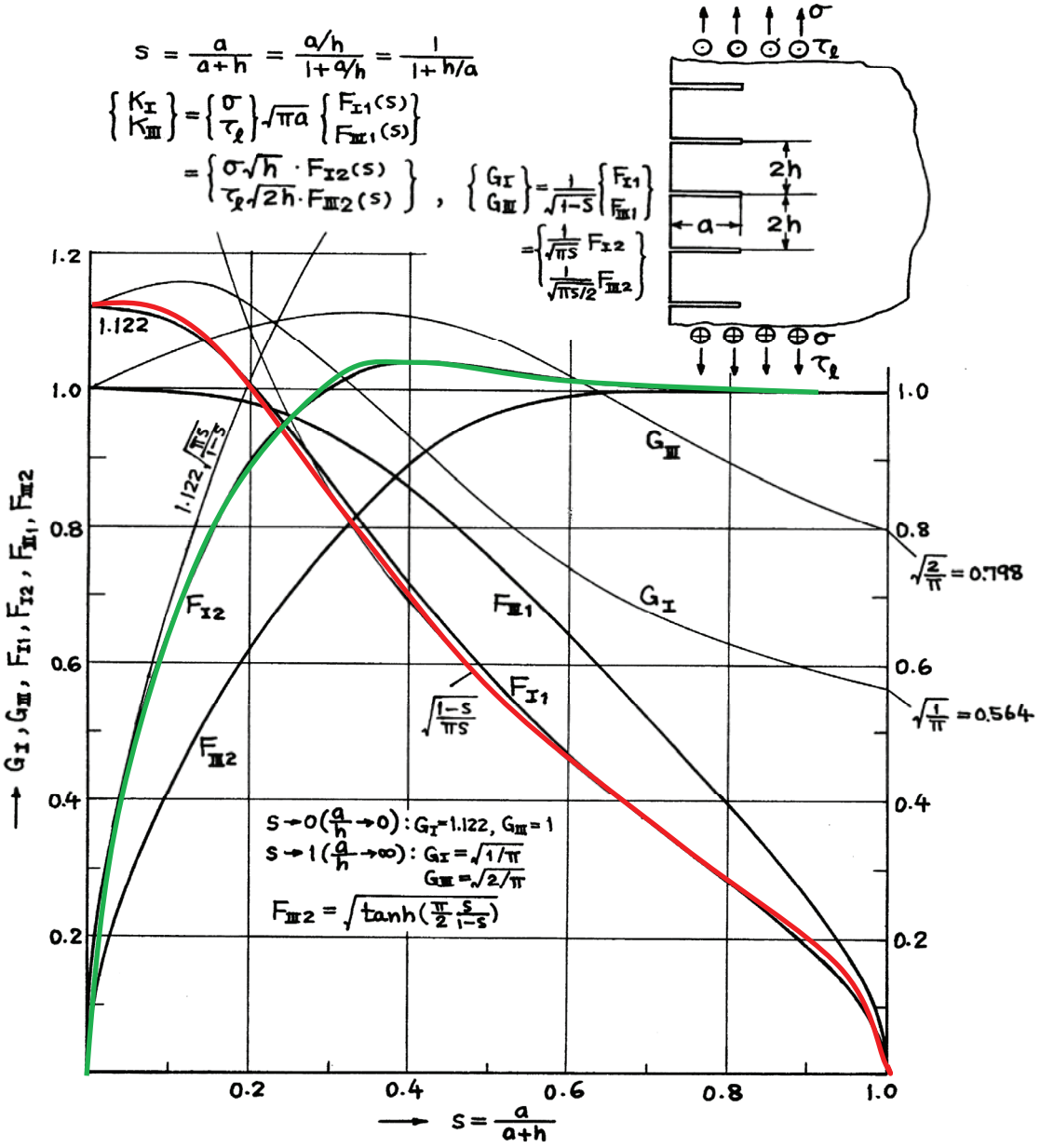

Figure 1. Periodic crack array geometry and results reported by Tada [17].

Methodology

The work is based on two primary components; finite element analysis and fracture mechanics. The FEA is used to estimate stress intensity factor solutions for a range of SCC crack in pipe geometries. The fracture mechanics is to demonstrate how the FEA results compare with the Tada work [17], and how these results can be leveraged for improved integrity program efficiency.

https://doi.org/10.52202/072781-0067

Finite Element Analysis (FEA)

The FEA work was performed primarily using ABAQUS software [19].

A standard pipe geometry was selected for the analyses; diameter 508 mm, wall thickness 10 mm and internal pressure of 1 MPa. Note that the analyses were all static elastic, so grade and toughness properties were not specified.

A series of models were constructed to investigate a range of crack depths and spacings. Depths ranged from 0.05 mm to 6.65 mm. Spacings ranged from 1.1 mm to 17.7 mm. Crack depth and spacing combinations were selected to explore the ratio between 0.1 and 0.6 to allow comparison to the Tada [17] work provided as the curves in **Figure 1**. An additional series of tests cases were performed to approximate a single, isolated crack. Note that by using a finite wall thickness, rather than the semi-infinite space of Tada [17], there is an additional parameter to consider.

The models were constructed to take advantage of symmetry. A small segment of the pipe circumference of 0.25° to 4° was modelled using 2D four-noded bilinear plain strain elements for each test case. Boundary conditions are shown in the figure below. A crack was modelled in the circumferential centre of the segment on the external pipe surface. Pressure was applied to the internal surface of the model.

Each test case represents a cross-section of the pipe, effectively modelling an infinitely long flaw with no consideration for crack length. The symmetry planes effectively simulate a periodic crack array, with the crack colonies extending all the way around the circumference of the pipe. This does not allow modelling of SCC cracks at the edge of a finite sized colony. Results should be considered accordingly.

Figure 2 shows a representative FEA model, illustrating the basic set-up, boundary constraints and loads. Boundary constraints are shown on the top and bottom surfaces of the model. Pressure is applied along the internal pipe surface on the left face of the model. Although the model appears rectangular, it is wedge-shaped, slightly narrower on the left side (internal pipe surface).

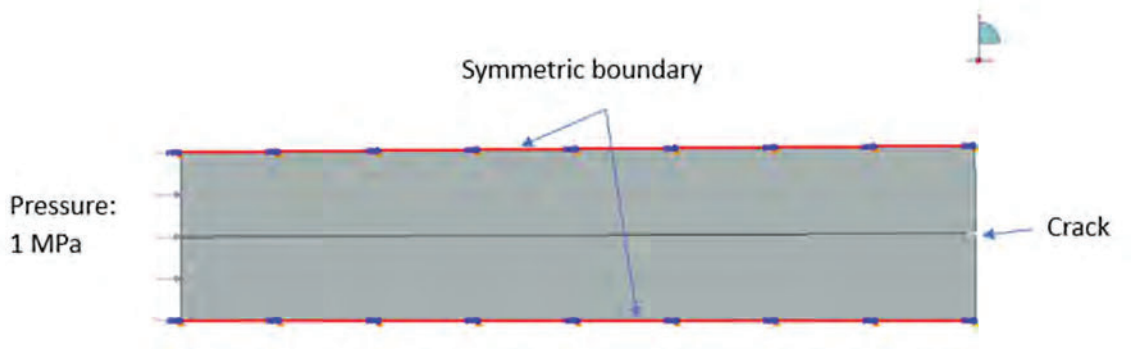

Figure 2. A representative FEA model showing the basic set-up, boundary constraints and loads.

https://doi.org/10.52202/072781-0067

A total of forty-seven test cases were run. A script was written in Python to allow batch processing. The models were solved using reduced integration and hourglass control. Results were spot checked by examining the resulting stress distributions from a random selection of test cases. Due to the powerful batch processing using Python scripting, the models were constructed with a refined mesh for all simulations and accuracy. Typical mesh sizing at the crack tips was in the order of 0.010 mm. The results are considered sufficient to assess trends, but further work may be required for engineering critical assessment.

Fracture Mechanics

The primary results of interest from the modelling are the calculated stress intensity factors, as a function of crack depth, crack depth ratio with respect to wall thickness, and crack half-spacing. These results were compiled for further evaluation. Plots of compliance factors, both standard F1 and modified F2, were constructed for comparison to the Tada [17] work.

Results

Finite Element Analysis

Preliminary studies suggested that stress intensity factors associated with deep cracks approaching the back-wall of the pipe internal surface deviated from textbook analytical solutions based on a simplified loading scenario. This prevented study of spacing ratios beyond s = 0.6. As such, the results reported here do not span the full range of parameters reported by Tada [17]. Trends may be inferred from the plots provided. Deeper flaw analysis will be considered for future study.

Figure 3 shows a stress distribution for one of the test cases for the single crack geometry. The boundaries of the models were examined to confirm appropriate application of the displacement conditions. The stress distribution at the crack tip was examined for symmetry and compared to textbook solutions [21].

Figure 4 and **Figure 5** show stress distributions for two of the test cases for closely spaced cracks in colonies. In these cases, the spacing is approximately 2 mm, comparable to a typical SCC colony spacing. The first distribution shows the zone of higher stress is concentrated into a small area at the shallow crack tip. Theoretically the stress is infinite at the crack tip and the zone extends in distance approximately one-half of the crack depth. The small zone does not infringe on the boundary of the model, indicating negligible shielding between neighbouring cracks. The second distribution shows the zone of higher stress spread to a large area ahead of the deeper crack tip. In this case, the stress concentration infringes on the boundaries of the models, indicating neighbouring cracks influence each other (through the symmetry plane) and this results in crack shielding. The flanks of the crack show zero stress, indicating the steel surface of the pipe is carrying no load. This dissipates the stress intensity along the tips of the multiple cracks in the colony.

https://doi.org/10.52202/072781-0067

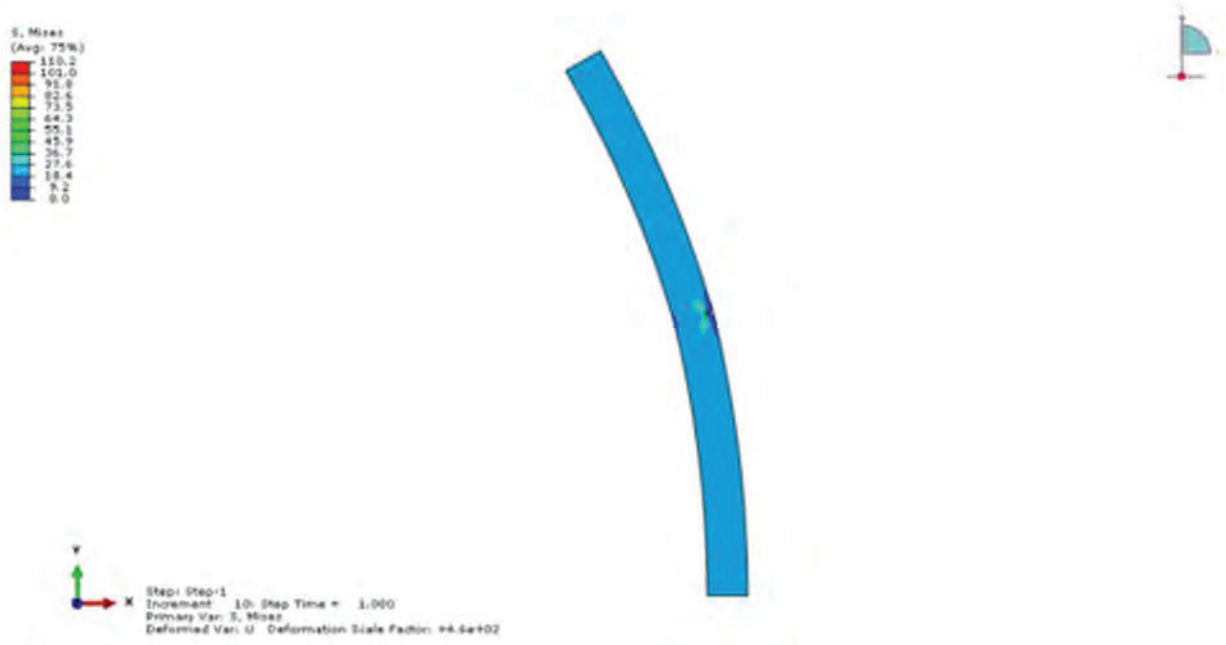

Figure 3. The resulting stress distribution for one of the test cases with a single crack. The KI stress intensity for this test case is expected to approximately match the theoretical stress intensity for a single flaw.

Figure 4. The resulting stress distribution for a test case with a shallow crack. The stress concentration zone does not reach the model symmetry boundary and there is negligible decrease in KI relative to the single crack case.

https://doi.org/10.52202/072781-0067

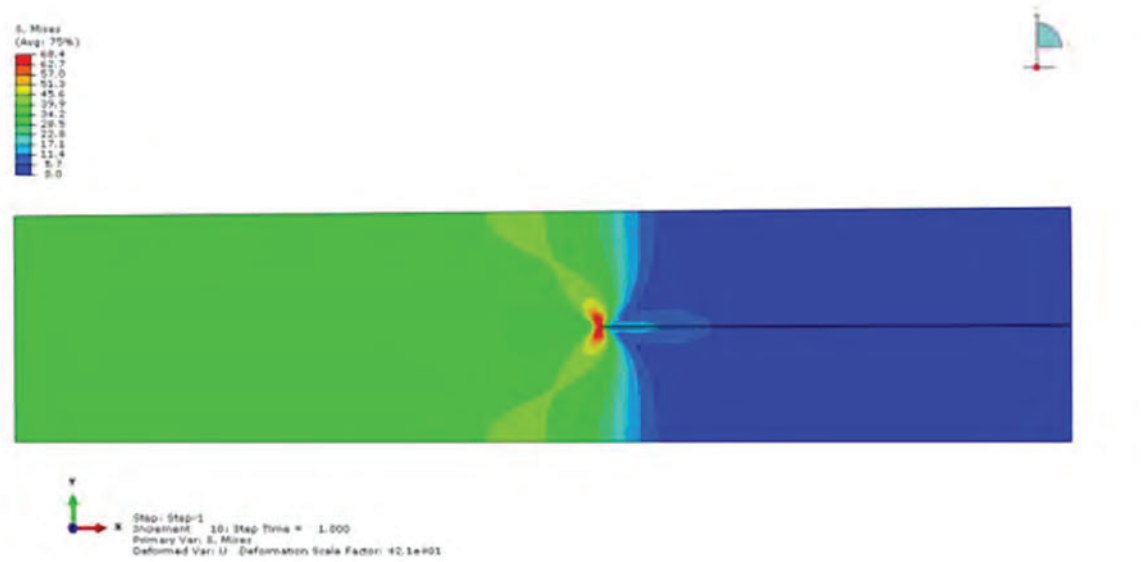

Figure 5. The resulting stress distribution for one of the test cases with a deep crack. The stress concentration zone does reach the model symmetry boundary and there is a significant decrease in the KI due to crack shielding.

Fracture Mechanics

The results of the FEA were compiled to construct plots of the compliance factor, both standard and modified versions.

Figure 6 is a plot of the standard compliance factors (F1) back - calculated from the FEA estimated stress intensities. This plot can be compared to the red curve in **Figure 1**. The red curve in **Figure 6** represents the standard compliance factor for a crack in an SCC colony with a spacing of 1.1 mm, a relatively tight spacing. The compliance factor decreases as the crack depth increases due to the shielding effect. This is consistent with the work of Tada [17]. The family of curves of different colours represents crack growth in SCC colonies with wider spacings. As the crack spacing increases, the standard compliance factor decreases at a slower rate, and then increases as the crack depth reaches midwall. This is inconsistent with the work of Tada [17], as the family of curves do not overlap. The difference in these cases is that the back-wall of the finite thickness pipe wall comes into play. Tada [17] considered semi-infinite space. These results must consider not just the ratio of the crack depth to crack spacing, but also the ratio of crack-spacing to pipe wall thickness. There is a clear effect for spacing narrower or wider than the pipe wall.

https://doi.org/10.52202/072781-0067

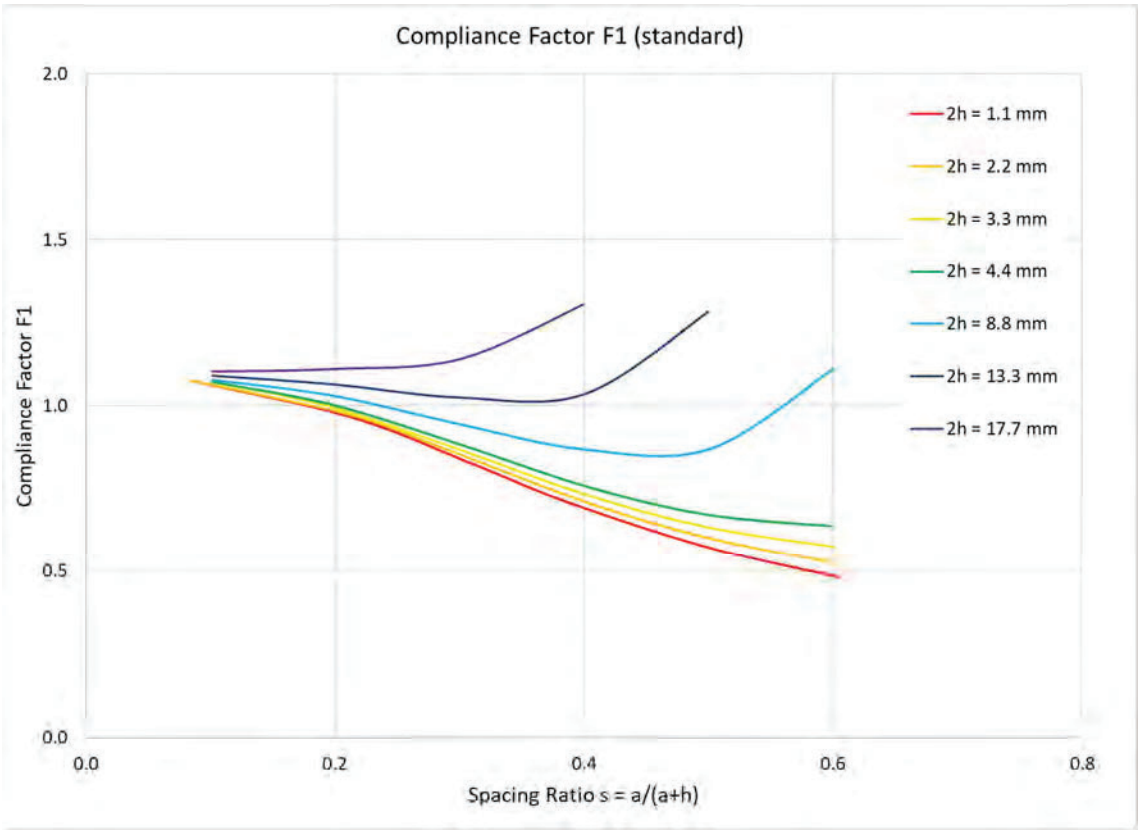

Figure 6. Plot of compliance factor F1 as a function of crack spacing parameter "s".

Figure 7 is a plot of the modified compliance factors (F2) back - calculated from the FEA estimated stress intensities. This plot can be compared to the green curve in **Figure 1**. The red curve in **Figure 6** represents the modified compliance factor for a crack in an SCC colony with a spacing of 1.1 mm, a relatively tight spacing. The compliance factor increases as the crack depth increases up to a spacing ratio of 0.3. This is consistent with the work of Tada [17], though the curve flattens slightly earlier. The curve plateaus to a spacing ratio of approximately 0.5. The stress intensity does not increase over this range, meaning that there is no mechanical driving force for crack growth. The cracks become thermodynamically meta-stable. The simulations correspond to crack depths between approximately 0.25 and 1 mm. This is consistent with field observations of crack dormancy [15,16].

The family of curves of different colours represents crack growth in SCC colonies with wider spacings. As the crack spacing increases, the modified compliance factor increases at a quicker rate. Again, there is an increase at midwall due to the back-wall approach. The cracks behave increasingly as single, isolated cracks as the spacing increases.

https://doi.org/10.52202/072781-0067

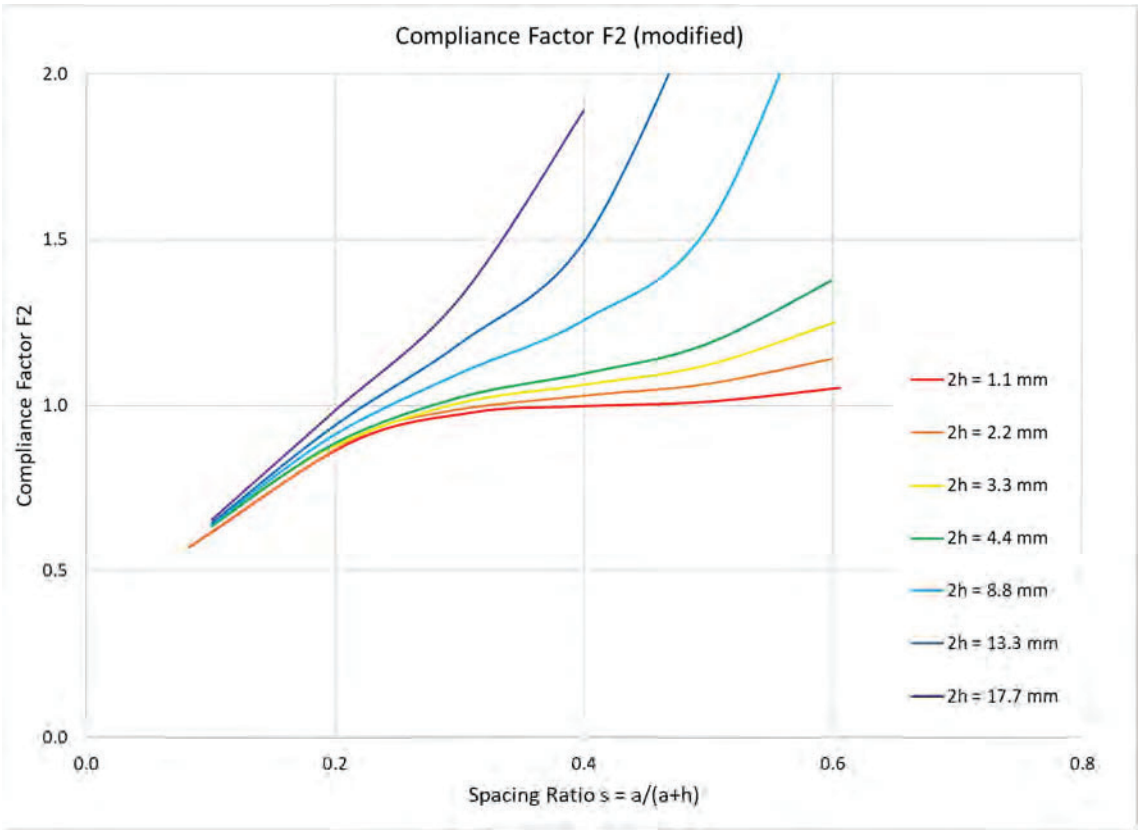

Figure 7. Plot of compliance factor F2 as a function of crack spacing parameter "s".

Figure 8 is a plot of the stress intensity factors as a function of crack depth for the various cracks spacings. This allows comparisons to the single crack solution. The stress intensities for the crack colonies are all lower than the single crack solution, and clearly depend on the spacing ratio. The cracks in the more tightly spaced colonies (red, orange and yellow curves) show negligible change along its length after initiation, consistent with the crack dormancy discussed above. The cracks in the more loosely spaced colonies (blues and purple curves) approach the behaviour of the single crack.

Discussion

The results of the FEA and plotting of stress intensity factors for crack colonies provide for several comparisons to be made amongst this work, the work of Tada [17], the work of Parker [18], and field observations. Note that these analyses are independent of SCC growth mechanism, there is no discussion of differences between near neutral pH or high pH conditions, as the study is purely an analysis of fracture mechanics.

https://doi.org/10.52202/072781-0067

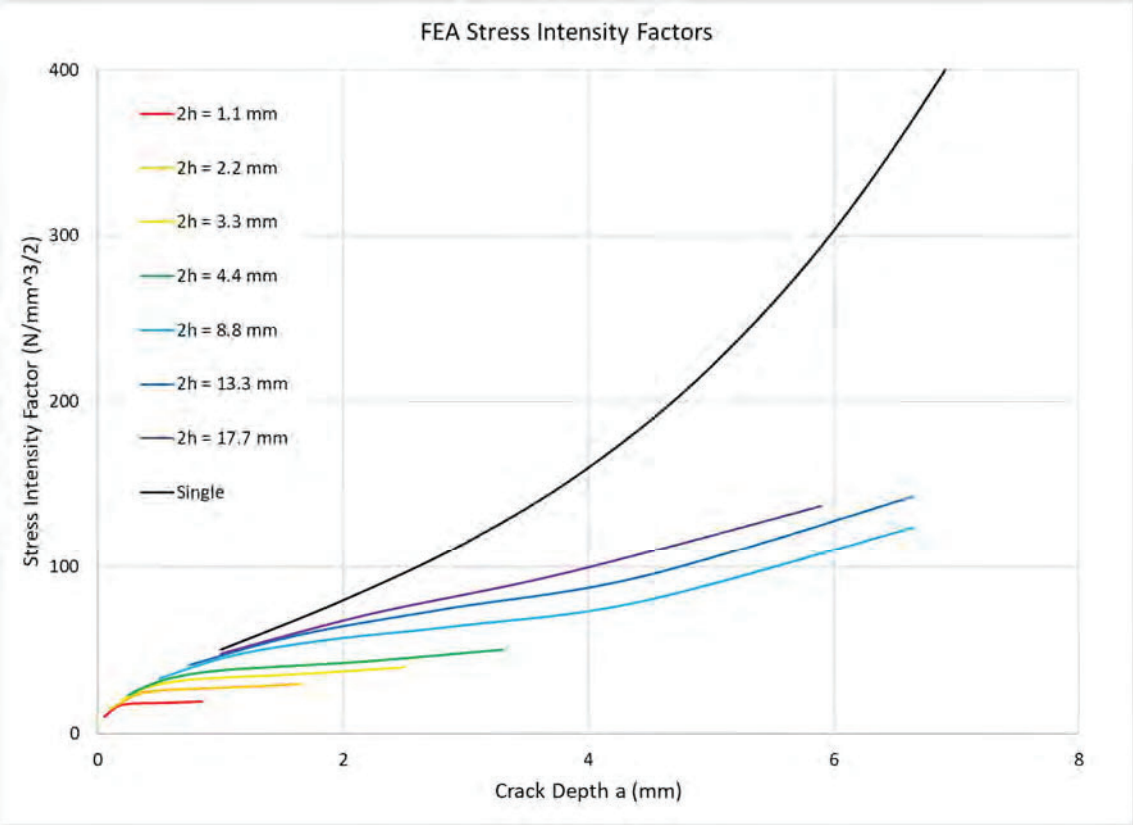

Figure 8. Plot of stress intensity factor as a function of crack depth "a".

Several studies have been performed by industry that examine crack dormancy [15,16,18,20]. Some researchers consider phases of crack growth and have used their observations to construct the bathtub model of crack growth. Several mechanisms have been proposed to explain crack slowing and dormancy, including crack blunting due to corrosion or creep exhaustion, or kinetic factors around diffusion of species between pipe surface and crack tip. These mechanisms do not explicitly consider the stress intensity factors associated with crack colonies, though some explanations have broadly been attributed to crack shielding. The stress intensity factors presented here suggest that crack dormancy can be attributed to fracture mechanics conditions alone.

Parker [18] completed a closely related study of periodic crack arrays. He used the Tada work, and specifically the prediction of crack dormancy at a spacing ratio of s = 0.4 (a/2h = 1/3) in **Figure 1**, to explain crack patterns in several disparate material systems. He proposed that periodic cracks would propagate to a depth of 1/3 their spacing and then go dormant. It could be argued that SCC cracks are known to propagate further and result in catastrophic pipeline failures. Parker extended his argument by discussing the concept of crack "shedding". He proposed that if the periodic crack array was subject to sufficiently high stresses, then 2/3 of the cracks would remain dormant, and 1/3 of the cracks would "break away" from the shielding effect and continue to propagate. This is consistent with researchers and pipeline owners who have reported re-initiating growth of dormant cracks through raising of operating pressures. The advancing cracks would then go dormant when the spacing ratio of the secondary cracks reached 1/3, and the cycle would continue. Parker [18] predicted a regular pattern of depth and crack spacing which he observed in mud-cracking, crevasse formation in glaciers, cooling of basalt columns and environmental cracking in gun tubes.

https://doi.org/10.52202/072781-0067

Figure 9 is a micrograph of periodic cracking in a gun tube [18]. Note the regular pattern in the depths of the cracks and their spacings. The two deepest cracks in the micrograph are approximately 1/3 the spacing between them. Two moderate cracks are observed, 1/3 the depth of the deeper cracks, and equally spaced. The shallowest micro-cracks are again 1/3 the depth of the moderate cracks and evenly spaced. The 1/3 ratio pattern is consistent in the crack depths and spacing.

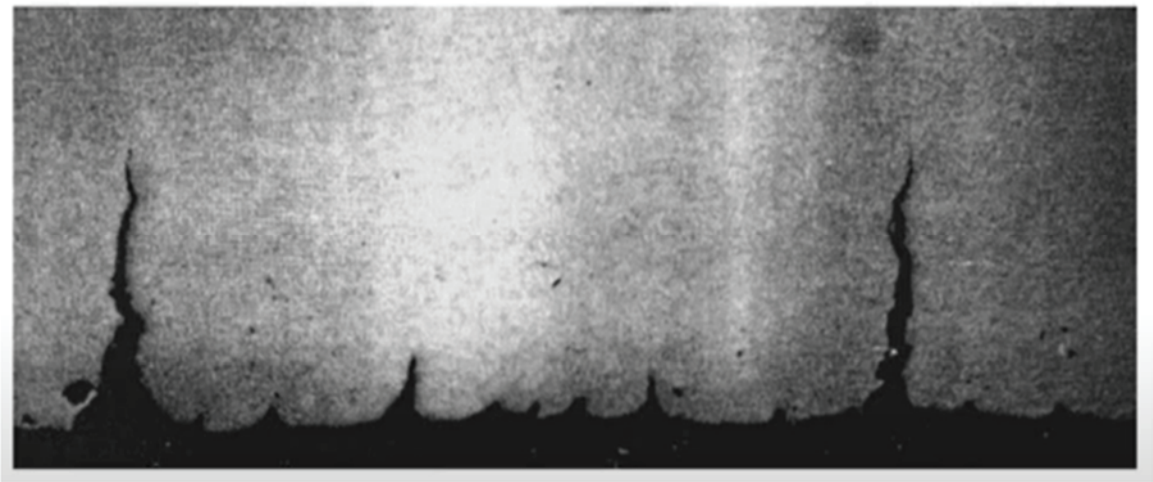

Figure 9. Micrograph of edge cracking in a gun tube, Figure 10 Reference [18]

Figure 10 is a micrograph of a metallographic cross-section through a pipe section subject to an SCC failure [20]. Note the regular pattern in the depths of the cracks and their spacing. The pattern is not perfect, but sufficiently close to the predicted 1/3 ratio to provide evidence in support of the work of Tada and Parker [17,18]. In addition, the stress intensity factor solutions estimated by this study are consistent.

Figure 10. Micrograph of a metallographic cross-section taken through a failed section of pipe, Figure T-4 Reference [20].

The regular depth and spacing pattern observed in the gun tube and failed SCC colony suggest the stress intensity reduction associated with shielding and predicted by Tada and Parker is a real effect. And this is consistent with predicted failure pressures being overly-conservative with respect to laboratory, hydrotest and in-service failure data.

The authors propose that understanding the lower stress intensity factors can be leveraged to improve the efficiency of pipeline integrity programs. Clearly, further work should be completed, as the above

https://doi.org/10.52202/072781-0067

study only provides estimates, and not sufficient for detailed engineering critical assessments. The lead author recently published studies that suggest the improvement in efficiency may be significant and relatively easily managed [11-14]. Several methodologies can be considered. One is to redefine stress intensity factors currently being used by industry and apply these to approved failure pressure models. An alternative would be to modify the critical stress intensity factors of materials used in assessments, to reflect a higher "effective" toughness. It is also possible to redefine an effective crack depth, and then continue to use current industry methodologies. These various approaches have their individual pros and cons. This is an area for further work.

Conclusions

This work has used FEA to estimate stress intensity factors in cracks in SCC colonies. Estimates show a dependence on the crack colony spacing, which is consistent with previous industry literature, and with the finite thickness of the pipe. The results indicate considerable reduction in stress intensity factors for cracks in closely spaced colonies, reflecting crack shielding. The results are consistent with previous studies and observations of crack dormancy in SCC colonies. As spacing widens the cracks are expected to behave similar to a single, isolated crack. These results are consistent with intuitive expectations. This study is intended as a proof-of-concept and further modelling would be required to use FEA derived stress intensity factors for detailed engineering critical assessments.

https://doi.org/10.52202/072781-0067

References

1. Kiefner, J.F., Maxey, R. J., Eiber, R. J., and Duffy, A. R., "Failure Stress Levels of Flaws in Pressurized Cylinders", ASTM STP536-EB/July 1973.
2. Kiefner, J. F., "Modified Ln-Secant Equation Improves Failure Prediction" Oil and Gas Journal (2008) 64-66.
3. ASME FFS-1 / API 579, "Fitness-for-Service", June 2016.
4. British Standard Institution 7910, "Guide to Methods for Assessing the Acceptability of Flaws in Metallic Structures", London, UK, 2013.
5. Corrosion Lifetime Assessment Software, CorLAS™, CC Technologies Inc. (now DNV GL), Dublin Ohio.
6. Anderson, T. L., "Development of a Modern Assessment Method for Longitudinal Seam Weld Cracks", PRCI PR-460-134506-R01, January 2015.
7. Rothwell, A. B. and Coote, R. I., "A Critical Review of Assessment Methods for Axial Planar Flaws", Ostende Pipeline Conference, 2009.
8. Yan, Z., Zhang, S., and Zhou, W., "Model Error Assessment of Burst Capacity Models for Energy Pipelines Containing Surface Cracks", International Journal of Pressure Vessels and Piping 120-121 (2014) 80-92.
9. Anderson, T. L., "Assessing Crack-like Flaws in Longitudinal Seam Welds: A State-of-the-Art Review", PRCI PR-460-134506, March 2017.
10. Yan, J., Zhang, S., Kariyawasam, S., Pino, M., and Liu, T., "Validate Crack Assessment Models with In-Service and Hydrotest Failures", IPC2018-78251, Calgary, 2018.
11. Scott, C., "Validation of the New Gamma Exponent Model for Axial Crack Assessment in Oil and Gas Pipelines", ASME PVP Virtual Conference 2020.
12. Scott, C., "A Statistical Analysis of the Gamma Exponent Model; a New Methodology for Corrosion Assessment of Localized Metal Loss and Stress Corrosion Cracking in Oil and Gas Pipelines", Paper 16368 NACE Virtual Conference 2021.
13. Scott, C., "Further Development of the Gamma Exponent Model for Assessment of Flaws in Oil and Gas Pipelines", JPSE 1 (2021) 321-328.
14. Scott, C., "The Impact of Failure Pressure Accuracy and Precision on Integrity Management and Decision Making", Pipeline Pigging and Integrity Management Conference, Houston TX, February 2022.
15. USDOT Office of Pipeline Safety, Technical Task Order 8, "Stress Corrosion Cracking Study, Final Report", January 2005.
16. "Stress Corrosion Cracking, Recommended Practices, Second Edition", Canadian Energy Pipeline Association, December 2007.
17. Tada, H., Paris, P., and Irwin, G., "The Stress Analysis of Cracks Handbook, Third Edition", ASME Press, New York, 2000.
18. Parker, A., "Stability of Arrays of Multiple Edge Cracks", Engineering Fracture Mechanics 62 (1999) 577-591.
19. ABAQUS – Finite Element Analysis Software
20. Wenk, R. L., "Field Investigation of Stress Corrosion Cracking", Pipeline Research Committee of the American Gas Association, 5th Symposium on Line Pipe Research, November 1974.
21. Anderson, T. L., "Fracture Mechanics Fundamentals and Applications, Fourth Edition" CRC Press Taylor and Francis Group 2017.

https://doi.org/10.52202/072781-0067